




Predicting epiglottic collapse in patients with obstructive sleep apnoea

Ali Azarbarzin¹, Melania Marques^{1,2}, Scott A. Sands^{1,3}, Sara Op de Beeck⁴, Pedro R. Genta², Luigi Taranto-Montemurro ¹, Camila M. de Melo^{1,5}, Ludovico Messineo¹, Olivier M. Vanderveken^{4,6}, David P. White¹ and Andrew Wellman¹

Affiliations: ¹Division of Sleep and Circadian Disorders, Brigham and Women's Hospital and Harvard Medical School, Boston, MA, USA. ²Pulmonary Division, Heart Institute (InCor), Hospital das Clínicas HCFMUSP, Faculdade de Medicina, Universidade de São Paulo, São Paulo, Brazil. ³Dept of Allergy Immunology and Respiratory Medicine and Central Clinical School, The Alfred and Monash University, Melbourne, Australia. ⁴Translational Neurosciences, Faculty of Medicine and Health Sciences, University of Antwerp, Antwerp, Belgium. ⁵Dept of Psychobiology, Universidade Federal de São Paulo (UNIFESP), São Paulo, Brazil. ⁶Dept of ENT, Head and Neck Surgery, Antwerp University Hospital, Edegem, Belgium.

Correspondence: Ali Azarbarzin, Sleep Disordered Breathing Lab, 221 Longwood Avenue, Boston, MA 02115, USA. E-mail: aazarbarzin@bwh.harvard.edu

 @ERSpublications

Epiglottic collapse can be identified from airflow characteristics during sleep <http://ow.ly/IafB30dbD60>

Cite this article as: Azarbarzin A, Marques M, Sands SA, *et al.* Predicting epiglottic collapse in patients with obstructive sleep apnoea. *Eur Respir J* 2017; 50: 1700345 [<https://doi.org/10.1183/13993003.00345-2017>].

ABSTRACT Obstructive sleep apnoea (OSA) is characterised by pharyngeal obstruction occurring at different sites. Endoscopic studies reveal that epiglottic collapse renders patients at higher risk of failed oral appliance therapy or accentuated collapse on continuous positive airway pressure. Diagnosing epiglottic collapse currently requires invasive studies (imaging and endoscopy). As an alternative, we propose that epiglottic collapse can be detected from the distinct airflow patterns it produces during sleep.

23 OSA patients underwent natural sleep endoscopy. 1232 breaths were scored as epiglottic/nonepiglottic collapse. Several flow characteristics were determined from the flow signal (recorded simultaneously with endoscopy) and used to build a predictive model to distinguish epiglottic from nonepiglottic collapse. Additionally, 10 OSA patients were studied to validate the pneumotachograph flow features using nasal pressure signals.

Epiglottic collapse was characterised by a rapid fall(s) in the inspiratory flow, more variable inspiratory and expiratory flow and reduced tidal volume. The cross-validated accuracy was 84%. Predictive features obtained from pneumotachograph flow and nasal pressure were strongly correlated.

This study demonstrates that epiglottic collapse can be identified from the airflow signal measured during a sleep study. This method may enable clinicians to use clinically collected data to characterise underlying physiology and improve treatment decisions.

This article has supplementary material available from erj.ersjournals.com

Received: Feb 17 2017 | Accepted after revision: June 21 2017

Copyright ©ERS 2017

Introduction

Obstructive sleep apnoea (OSA) is a common disorder characterised by recurrent upper airway collapse during sleep [1], which causes sleep fragmentation [2] and sympathetic activation [3]. A number of drug-induced sleep endoscopy (DISE) studies in OSA patients have demonstrated that the upper airway obstruction results from the collapse of one or more pharyngeal structures, such as the soft palate, the lateral pharyngeal walls, the tongue base and/or the epiglottis [4–6].

DISE studies, which visualise epiglottic collapse better than traditional imaging techniques, have shown that epiglottic collapse occurs more often than previously described [6–8]. In fact, some studies have reported that up to 30% of patients have complete collapse of the epiglottis [7]. Research also indicates that epiglottic collapse is difficult to treat with conventional therapies, such as oral appliances [9] and even continuous positive airway pressure (CPAP) [10, 11]. Therefore, recognising whether and how often a patient's upper airway collapses at the epiglottis could have important implications for treatment.

To determine whether epiglottic collapse contributes to OSA in a given patient, imaging techniques (e.g. computed tomography [12] and magnetic resonance imaging [13]) and DISE studies have been utilised. However, the invasive and expensive nature of these procedures hampers routine assessment of the structure causing collapse in the clinical setting. As an alternative approach, it has been shown that individuals with OSA exhibit well-defined, reproducible intrabreath airflow characteristics during sleep [14, 15]. Our group has noted a link between one of these characteristics (the magnitude of negative effort dependence, the reduction in airflow in association with increasing inspiratory effort) and the presence of epiglottic collapse in OSA [16]. In addition, our results suggested that rapid changes in inspiratory airflow within a breath (“discontinuities”), scored visually, were a recognisable hallmark of epiglottic collapse. However, to date, there has been no systematic investigation identifying epiglottic collapse from flow characteristics.

In this study, we hypothesised that epiglottic collapse has distinct and identifiable effects on the within-breath airflow shape during sleep in patients with OSA. We employed a machine-learning approach to develop and validate a model that uses flow characteristics (features) to predict the presence *versus* absence of epiglottic collapse as defined by gold standard endoscopy. Endoscopy was performed simultaneously with flow measurement during natural sleep. As an additional clinical validation, pneumotachograph flow and nasal pressure were measured simultaneously on a separate subgroup of patients. The correlations between pneumotach- and nasal pressure-measured features were assessed.

Methods

Participants

OSA patients (aged 21–70 years) with an apnoea–hypopnoea index (AHI) >10 events·h⁻¹ were invited to participate. The exclusion criteria included cardiac disease (uncontrolled hypertension or heart failure) or any other serious medical condition, and the use of medications known to influence sleep, respiration or muscle control. The study was approved by the Partners Healthcare institutional review board. All participants provided written informed consent prior to study enrolment. The patients' characteristics and baseline polysomnography parameters were analysed retrospectively.

Endoscopic studies

Measurements and equipment

Participants were instrumented for a physiological polysomnographic study. Electroencephalography (EEG), chin electromyography (EMG) and electro-oculography (EOG) were recorded for sleep staging. Piezoelectric bands around the chest and abdomen monitored respiratory movements/effort. ECG, body position and arterial oxygen saturation (SaO₂) were also recorded. In addition, participants wore a sealed nasal mask to facilitate airflow measurement using a pneumotach (Hans-Rudolph, Kansas City, MO, USA). Mask pressure was monitored using a pressure transducer (Validyne, Northridge, CA, USA) referenced to atmosphere. Pharyngeal lumen pressure was measured using a 5-French Millar catheter that

Support statement: This work was performed at the Brigham and Women's Hospital and Harvard Medical School and was supported by funding from Fan Hongbing, President of the OMPA Corporation, Kaifeng, China; a Philips Respironics research grant; National Institutes of Health grants (R01 HL 128658, 2R01HL102321 and P01 NIH HL095491); and the Harvard Catalyst Clinical Research Center (UL1 RR 025758-01). A. Azarbarzin was supported by the Natural Sciences and Engineering Research Council of Canada (NSERC). S.A. Sands was supported by the National Health and Medical Research Council of Australia (1053201), Menzies Foundation, the American Heart Association (15SDG25890059) and American Thoracic Society Foundation. L. Taranto-Montemurro is supported by the American Heart Association (17POST33410436). P.R. Genta and M. Marques were supported by FAPESP. Funding information for this article has been deposited with the Crossref Funder Registry.

Conflict of interest: Disclosures can be found alongside this article at erj.ersjournals.com

had six pressure sensors 0.75 cm apart starting at the tip (P_1 – P_6 (downstream pressure sensor, placed above the epiglottis)). To visualise the airway, a 2.8-mm diameter paediatric bronchoscope was inserted through the second nostril. Spike 2 software (Cambridge Electronic Design, Cambridge, UK) was used to acquire the physiological signals and endoscopic images. All signals except EEG, EMG, EOG and ECG (which were sampled at 125 Hz) were captured at a sampling frequency of 500 Hz, and the images were sampled at 30 frames·s⁻¹.

Protocol

Participants were asked to sleep in either the supine or lateral position. To evaluate which pharyngeal structure was causing collapse, the scope's tip was initially placed above the soft palate and several flow-limited breaths were recorded. Flow limitation was determined based on simultaneous observations of flow and epiglottic pressure (lack of increase in flow despite decreasing epiglottic pressures). The tip of the scope was then advanced to the oropharynx to visualise the oropharyngeal and hypopharyngeal structures. This process was repeated, with as many breaths observed at both pharyngeal levels as possible throughout the night. While the scope was in the airway the whole night, videos were only recorded intermittently due to the technical limitations involved with handling the extremely large video files (e.g. limited memory on the local computer). In addition, breaths were excluded from the analysis if 1) they occurred during wakefulness, rapid eye movement sleep or arousals; 2) they occurred during sleep in the lateral position, because the occurrence of epiglottic collapse substantially decreases in this position [17]; 3) they were not flow limited; or 4) secretions blurred the endoscopic view.

Breath visualisation and gold standard classification

All eligible breaths were labelled as being associated with epiglottic collapse or nonepiglottic collapse using the visual inspection of the videos captured by the scope (in the velopharynx and oropharynx) during natural sleep. The breaths were labelled as epiglottic collapse if the epiglottis appeared to completely (or almost completely, >90% obstruction) close in either the anteroposterior or lateral direction (see online supplementary material for videos of both types of collapse and their associated flow patterns). In addition, to confirm that the flow limitation was not due to collapse of structure(s) above the epiglottis, the pressure just above the epiglottis was inspected and compared to mask pressure (the waveforms resemble one another when the epiglottis collapses (figure 2)). This visual classification was performed by two investigators (MM and SO), with any discrepancies being resolved by a third investigator (AW).

Simultaneous measurements of pneumotachograph flow and nasal pressure

For validation, pneumotach flow and nasal pressure were measured simultaneously (using an oronasal mask) in a separate subgroup of patients. A modified single-ended nasal cannula was used to measure nasal pressure. One end of the nasal cannula was cut, sealed and taped inside the mask and the other end was taped and passed through a sealed port in the mask and connected to a pressure transducer (Validyne). The nasal pressure (unfiltered, direct-coupled) was referenced to the mask pressure to measure the pressure difference between the inside and outside of the nostrils. To obtain a more accurate estimate of the pneumotach flow, the nasal pressure signal (PN) was linearised by different transformations, including nasal pressure signal to the power of 0.75 ($V'PN^{0.75}$; see online supplementary material for more details). To obtain the correlation coefficients between pneumotach- and nasal pressure-measured variables, breaths were randomly selected from this subgroup of patients.

Machine learning and algorithm development

The algorithm development was performed independently by a separate investigator (AA) blinded to the visualisation and gold standard classification process. For each breath, 32 flow characteristics (features) were determined. The detailed calculations of these features are described in the online supplementary material. Briefly, the following important features were calculated. 1) Discontinuity index ($D1$), measured from the slope of the steepest line fitted to the inspiratory flow; 2) inspiratory jaggedness index (Ji) and expiratory jaggedness index (Je), which measure the extent of deviation from flatness in the inspiratory and expiratory flow (more variable flow results in a higher jaggedness index); 3) respiratory parameters: the ratio of within-breath respiratory variables, such as the ratio of mean inspiratory flow and tidal volume (V'_{mean}/V_T), the ratio of the time of peak expiration and total expiration time (t_{maxE}/t_e) and the ratio of peak expiratory flow and tidal volume (V'_{maxE}/V_T); 4) fluttering index, which quantifies the power of high-frequency variations in the inspiratory flow normalised by squared tidal volume (FPi/V_T^2).

Classification

Here we use a classifier (*i.e.* equation or model) to define a boundary, based on flow characteristics, that best discriminates between breaths with *versus* without epiglottic collapse. We employed an established

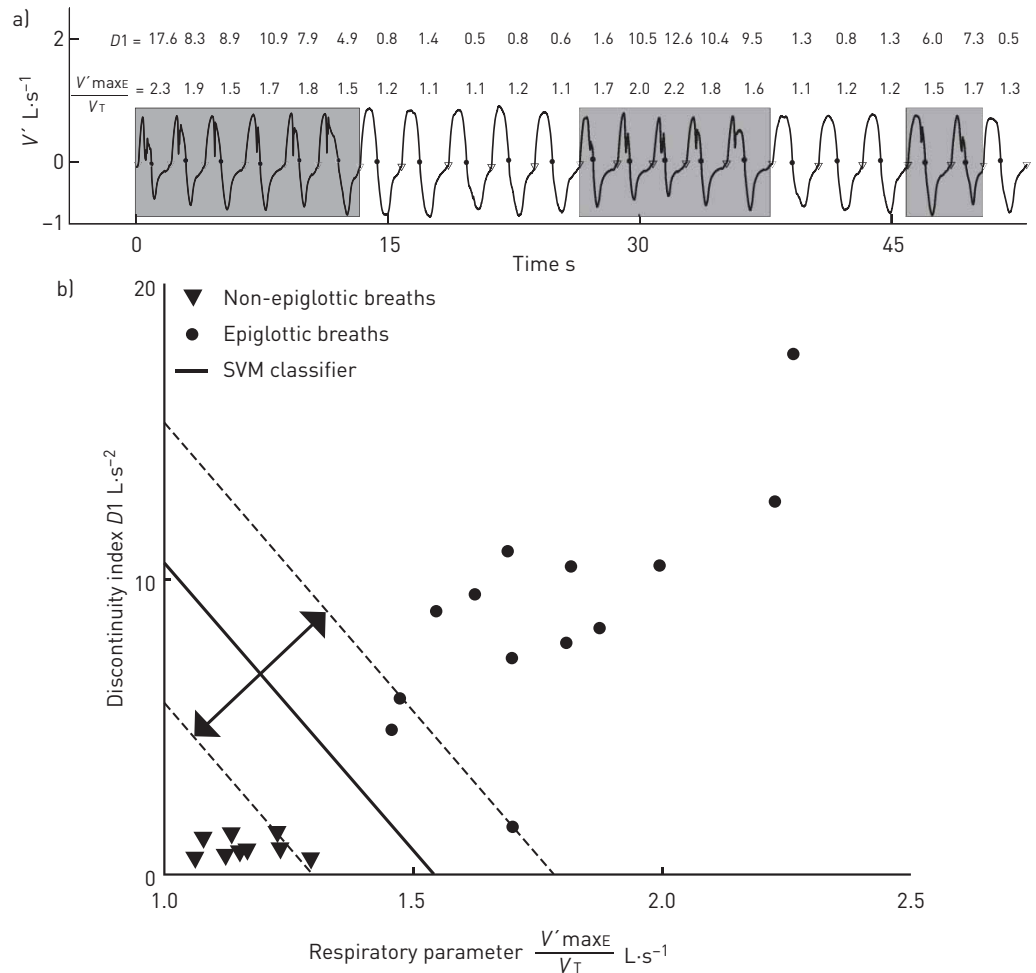


FIGURE 1 In this simplified example classification scheme (support vector machine (SVM)), 22 breaths are presented, 13 of which have epiglottic collapse. a) Two characteristics (features) are highlighted, the discontinuity index ($D1$) and respiratory parameter (peak expiratory flow [$V'_{\max E}$]/tidal volume [V_T]), and overlaid on the flow trace. b) Plot of characteristics for breaths with epiglottic collapse *versus* those without epiglottic collapse. The classifier finds a linear boundary between groups, which maximises the margin of error (arrows and dashed lines).

approach to develop and validate a classifier (supervised learning [18]) whereby a model is trained based on gold-standard classification (breath-by-breath endoscopic assessment) and tested in a set of data where the gold-standard classification is hidden (10-fold cross-validation). We used a “support vector machine classifier” which tends to outperform other types of classifiers [19–22]. Figure 1 shows an example implementation. In addition to the type of classifier, it is essential to select an optimal number of features to maximise the predictive value in the training and validation datasets. Adding more features may result in overfitting. To prevent overfitting, a sequential forward feature selection process [23] was performed within a 10-fold cross-validation [24] framework. Features were included in the model sequentially until there was no further improvement in predictive value based on the mean of sensitivity and specificity obtained from 10-fold cross-validation (*i.e.* $n=7$ features; see online supplementary material for a detailed description).

Statistical analyses

Data are expressed as mean \pm SD or median (25th–75th percentile) unless otherwise specified. Unpaired two-tailed t-tests or Wilcoxon signed rank tests were performed for between-group comparisons. In addition to model development and validation, we assessed whether breaths with epiglottic collapse were statistically associated with selected features using linear mixed model analysis [25, 26] (see online supplementary material for an example analysis). Statistical significance was accepted at $p<0.05$.

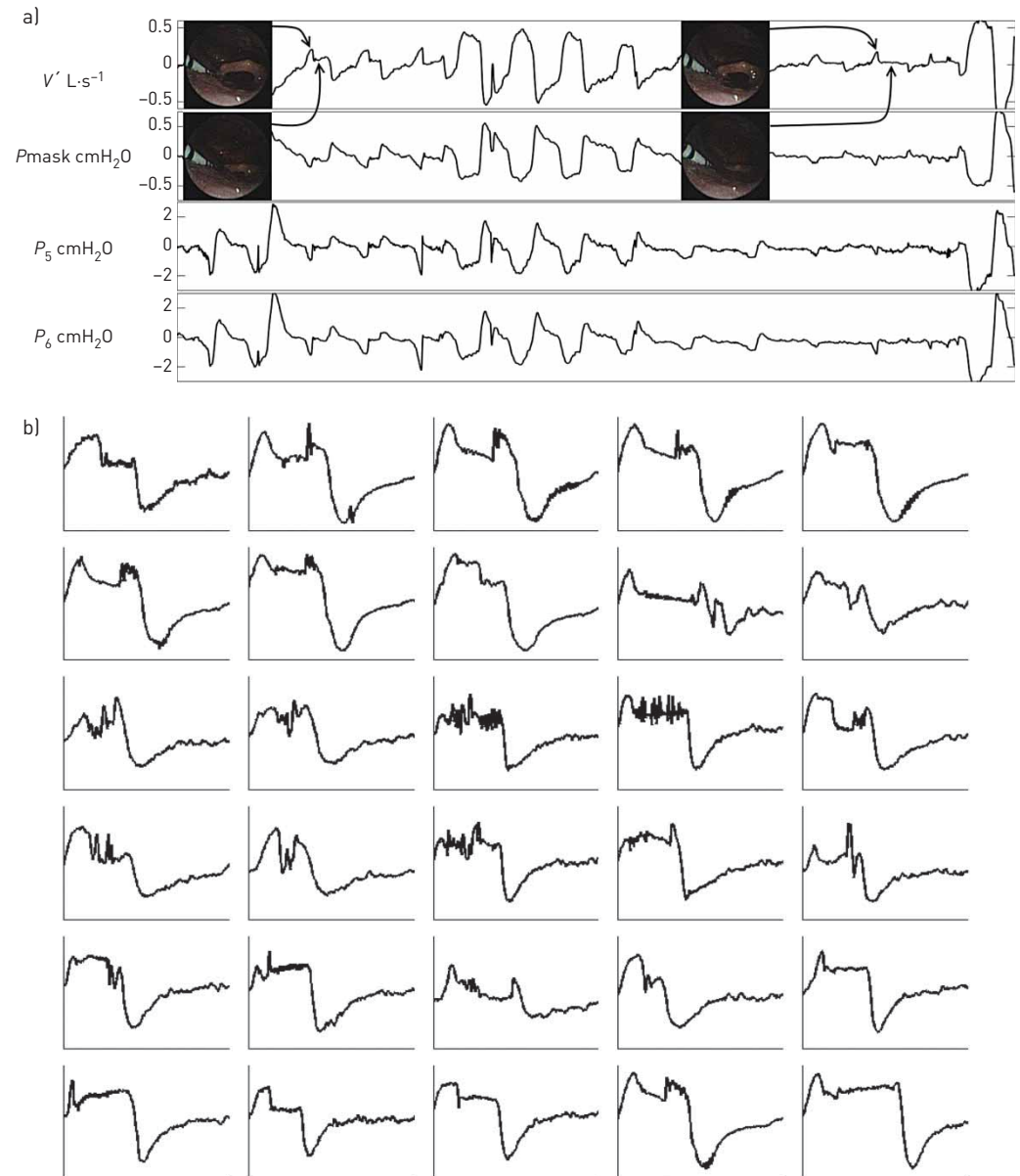


FIGURE 2 a) Epiglottic collapse accompanied by distinct flow characteristics (e.g. discontinuities in inspiratory flow). The pressure above the epiglottis (P_5 and P_6 , downstream to P_5) closely follows the mask pressure, confirming that the airway above the epiglottis is patent. b) Examples of epiglottic collapse associated with sudden flow change.

Results

Patient characteristics

The endoscopy study involved 23 OSA patients (age 49.9 ± 9.3 years; six females) with an AHI of 48.6 ± 30.4 events·h⁻¹ and a body mass index of 32.8 ± 6.0 kg·m⁻². In addition, 10 patients (age 57.2 ± 8.2 years; two females) with an AHI of 42.0 ± 25.5 events·h⁻¹ and a body mass index of 29.6 ± 6.5 kg·m⁻² were studied for simultaneous recording of pneumotach flow and nasal pressure. Tables 1 and 2 present the subjects' characteristics and polysomnography parameters.

Breaths verified by endoscopy

On average, 102 ± 48 min of endoscopy video per subject in the supine position were obtained. A total of 1232 flow-limited breaths (54 ± 61 breaths per subject) during supine non-rapid eye movement sleep were analysed (after excluding breaths during wakefulness, arousals, excessive saliva, improperly positioned scope or otherwise poor visualisation of the airway structures). From these breaths, using the visual

TABLE 1 Anthropometric parameters of patients

	Endoscopy physiology study				Nasal pressure study
	All subjects	Nonepiglottic collapse	Epiglottic collapse	p-value	
Subjects	23	18	5		10
Age years	49.9±9.3	47.8±8.7	57.4±7.6	0.038	57.2±8.2
Sex male:female	17:6	12:6	5:0	0.3 [#]	8:2
Neck circumference cm	40.7±4.5	40.7±4.9 [¶]	40.8±3.4	>0.9	41.5±3.4
BMI kg·m⁻²	32.8±6.0	33.0±5.8	32.1±7.2	0.8	29.6±6.5
Mallampati score	3.5±0.7	3.6±0.6 [*]	3.3±1.0 [*]	0.4	
Total endoscopy recording min	149.8±49.3	143.4±54.2	166.2±19.4	0.4	

Data are presented as n or mean±sd, unless otherwise stated. BMI: body mass index. [#]: evaluated using Fisher's exact test; [¶]: one data point is missing from the group; ^{*}: two data points are missing from the calculation.

inspection of endoscopy videos and pressure tracings, 244 (19.8%) were classified as epiglottic collapse, while 988 (80.2%) were classified as being associated with other sites of collapse.

Example traces

Figure 2 demonstrates example breaths that were associated with epiglottic collapse. The oropharyngeal view shows the epiglottis closing (or severely narrowing) at the beginning of inspiration, shown in figure 2a, resulting in an abrupt and severe reduction of airflow. This immediate reduction in airflow at the level of the epiglottis causes the upstream pressures (e.g. P₅ and P₆) to become positive and follow the mask pressure. It also produces a discontinuity feature in the inspiratory flow that manifests as a fast rate of change in flow and a jagged inspiratory pattern. Figure 2b shows several example breaths that were associated with epiglottic collapse. A common feature is the presence of a discontinuity in the inspiratory flow. Breaths without epiglottic involvement, shown in figure 3, clearly have different features, including fluttering and reduced jaggedness. In addition, the "pressure dissociation" between P₃ and P₆, both of which are upstream to the epiglottis, suggest that the choke point is between these two sensors, *i.e.* at the level of the palate or tongue base.

Feature selection using 10-fold cross-validation

Seven out of 32 features were selected by our algorithm. The selected features were the discontinuity index (D1), inspiratory jaggedness index (JI_i), expiratory jaggedness index (JI_e), mean inspiratory flow normalised by tidal volume (V'_{mean}/V_T), relative time of expiratory peak (t_{maxE}/t_e), inspiratory fluttering index (FP_i/V_T^2) and peak expiratory flow normalised by tidal volume (V'_{maxE}/V_T). The final cross-validated accuracy ((sensitivity + specificity)/2) was 84% (validation data). The classification accuracy (training) was 87% (sensitivity 96%, specificity 78%), indicating a loss of 3% in accuracy when tested on independent data.

TABLE 2 Polysomnographic parameters of patients

	Endoscopy physiology study [#]				Nasal pressure study
	All subjects	Nonepiglottic collapse	Epiglottic collapse	p-value	
Subjects	23	18	5		10
TST min	291±93 [¶]	286±99 [¶]	305±76 [¶]	0.7	306±70.9
Sleep efficiency %	70.4±14.4 [¶]	71.0±14.6 [¶]	68.5±15.0 [¶]	0.7	71.9±13.9
NREM 1 %TST	27.6±24.8 [¶]	27.0±26.4 [¶]	29.4±22.1 [¶]	0.9	28.2±20.1
NREM 2 %TST	57.0±20.2 [¶]	56.8±21.3 [¶]	57.6±18.5 [¶]	>0.9	56.2±16.3
NREM 3 %TST	1.5±2.9 [¶]	1.6±3.1 [¶]	1.0±2.3 [¶]	0.7	6.8±13.9
REM %TST	14.1±8.9 [¶]	14.8±8.5 [¶]	12.1±10.6 [¶]	0.6	8.8±6.0
AHI events·h⁻¹	48.6±30.4	51.1±33.0	40.7±20.8	0.5	42.0±25.5
Arl events·h⁻¹	43.0±31.3 [¶]	42.3±34.6 [¶]	45.3±20.3 [¶]	0.9	44.7±20.1
Nadir Sa_{o2} %	81.7±9.4 [¶]	83.1±8.4 [¶]	77.2±12.0 [¶]	0.2	83.4±12.5

Data are presented as n or mean±sd, unless otherwise stated. TST: total sleep time; NREM 1, NREM 2, NREM 3: non-rapid eye movement sleep stages 1–3; REM: rapid eye movement sleep; AHI: apnoea–hypopnoea index; ArI: arousal index; Sa_{o2}: arterial oxygen saturation. [#]: polysomnography data were analysed retrospectively; [¶]: two data points are missing from the calculation.

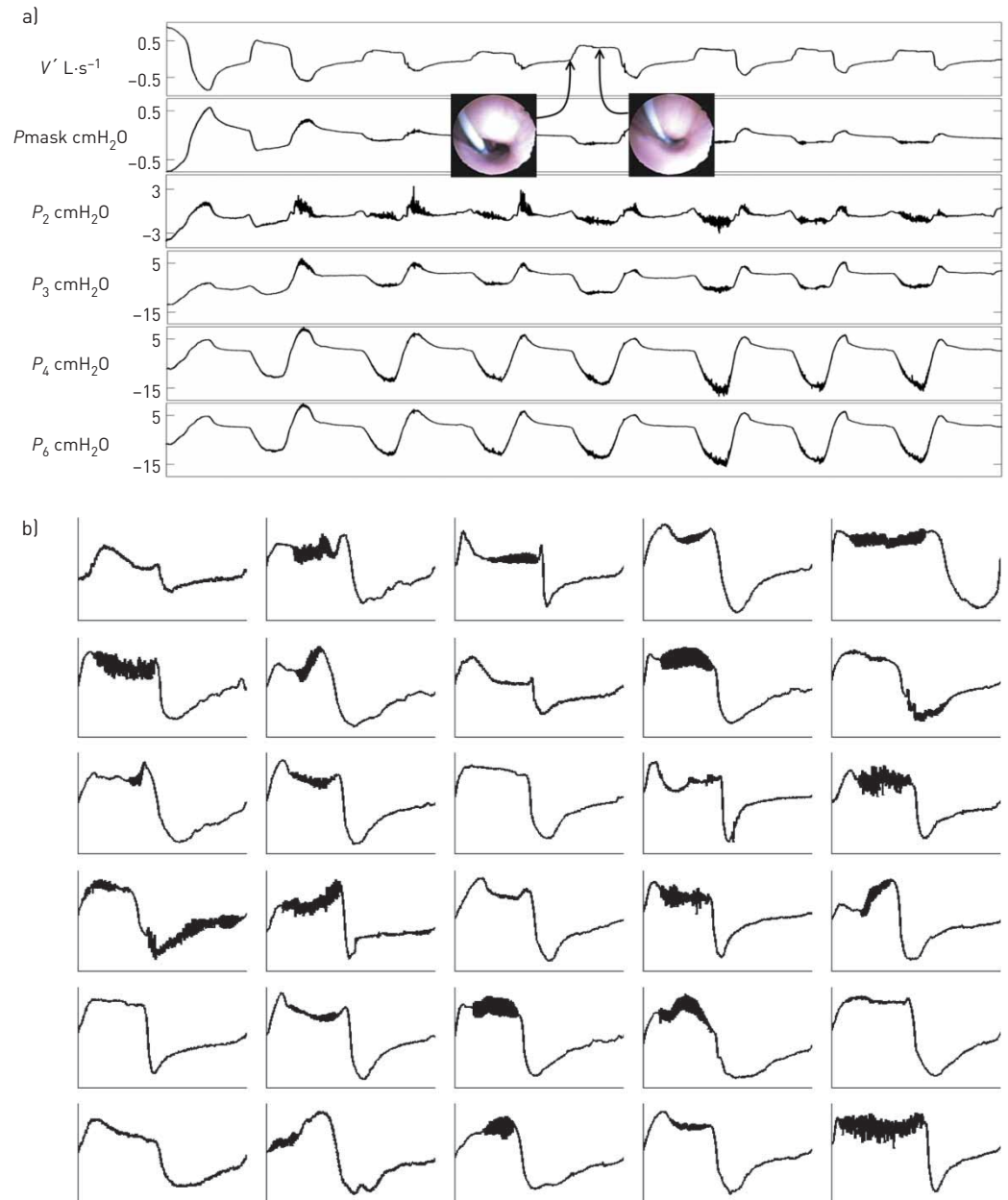


FIGURE 3 Nonpiglottic pharyngeal collapse often produces a “flat-top” flow shape. a) The multitip pressure tracings suggest that there is a choke point between P_3 and P_4 ; b) example traces of nonpiglottic collapse.

Even though a nonlinear combination of these seven features (online supplementary material) resulted in 84% cross-validated accuracy, the linear mixed model analysis revealed that epiglottic collapse was generally predicted by a higher $D1$ (2.2 ± 0.38 points larger for breaths associated with epiglottic collapse; $p = 8.0 \times 10^{-9}$) and a higher Ii (0.09 ± 0.02 points larger for epiglottic-related breaths; $p = 1.1 \times 10^{-4}$). Figure 4 displays an example of the flow patterns associated with small and large values of these two features. Complementary results involving feature selection and linear mixed model analyses have been described in the online supplementary material.

Validation against nasal pressure recordings

1768 breaths (177 ± 75 breaths per subject) were randomly selected from the polysomnography recordings that contained simultaneous measurements of pneumotach flow and nasal pressure (figure 5). Discontinuity indices obtained from pneumotach flow were strongly associated with their concurrent values obtained from nasal pressure (figure 6). The highest correlation was observed when flow was estimated by the nasal pressure to the power of 0.75 ($D1(V')$ versus $D1(V'_{PN}^{0.75})$): $r = 0.8$, $p = 0$; figure 6 and

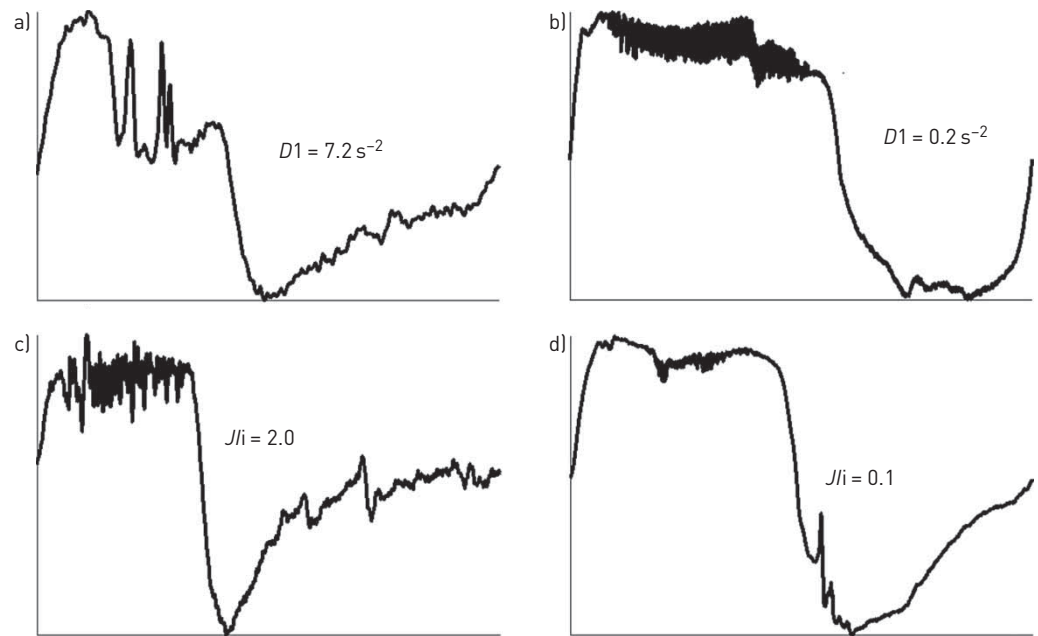


FIGURE 4 Large values of the discontinuity index $[D1]$ and the inspiratory jaggedness index $[Jli]$ predict epiglottic collapse. a, c) Flow patterns associated with high values of the discontinuity index and jaggedness index; b, d) flow patterns associated with low values of these features.

online supplementary material for correlation analysis involving different transformations). Similarly, there was a strong correlation between the inspiratory jaggedness index obtained from pneumotach flow and transformed nasal pressure ($Jli(V')$ versus $Jli(V'PN^{0.75})$): $r=0.94$, $p=0$; figure 6). Other features resulted in similar correlations, indicating that epiglottic collapse can be identified reliably from nasal pressure recordings performed in clinical sleep laboratories.

Discussion

The major conclusion of the current study is that epiglottic collapse produces flow features that 1) are different from the features produced by nonepiglottic-related obstructions; 2) are easy to quantify; and 3) can be reliably estimated from high-fidelity (unfiltered, DC-coupled amplification) nasal pressure signals collected during clinical sleep studies. The main predictors of epiglottic collapse were discontinuity and jaggedness. Additional regression analysis of the simultaneously measured flow and nasal pressure features revealed identity relationships (linear relationship with slope ≈ 1 and small intercept, correlation coefficients >0.8).

Prevalence and significance of epiglottic collapse

Previous studies have reported a wide variation in the prevalence of epiglottic collapse in OSA patients [6–8, 27]. This may be related to the inconsistent definition of epiglottic collapse in the literature. For instance, DA CUNHA VIANA *et al.* [27] reported that 42% of OSA patients had at least partial epiglottic collapse. However, when only obstructions with $>75\%$ narrowing were considered, epiglottic collapse was found in only 20% of the patients examined. In our study, only complete or nearly complete obstruction of the epiglottis was considered as epiglottic collapse. There were three reasons for classifying it this way. First, we noticed that partial epiglottic collapse (*e.g.* 50–75% narrowing) virtually never produced a measurable reduction in flow (figure 2 and the online supplementary video). Second, “complete” collapse was easier to score and led to near perfect inter-rater agreement. Finally, by restricting our definition to complete collapse, we felt more comfortable with categorising the epiglottis as a dominant cause of obstruction. Previous studies have argued that posterior movement of the tongue could cause the epiglottis to collapse [28]. However, this can be quite subjective and difficult to quantify endoscopically. Notably, in the many instances of epiglottic collapse examined in the current study, we often noticed the opposite, *i.e.* the tongue seemed to remain stationary or even move anteriorly slightly when the epiglottis collapsed. Future studies, in which the tongue contribution to epiglottic collapse can be more systematically quantified are needed to explore this further.

Discontinuity and jaggedness as a signature of epiglottic collapse

The literature shows that OSA patients exhibit distinct and characteristic flow limitation patterns during sleep [14, 15]. AITTOKALLIO *et al.* [15] found well-defined and reproducible flow shapes in different OSA

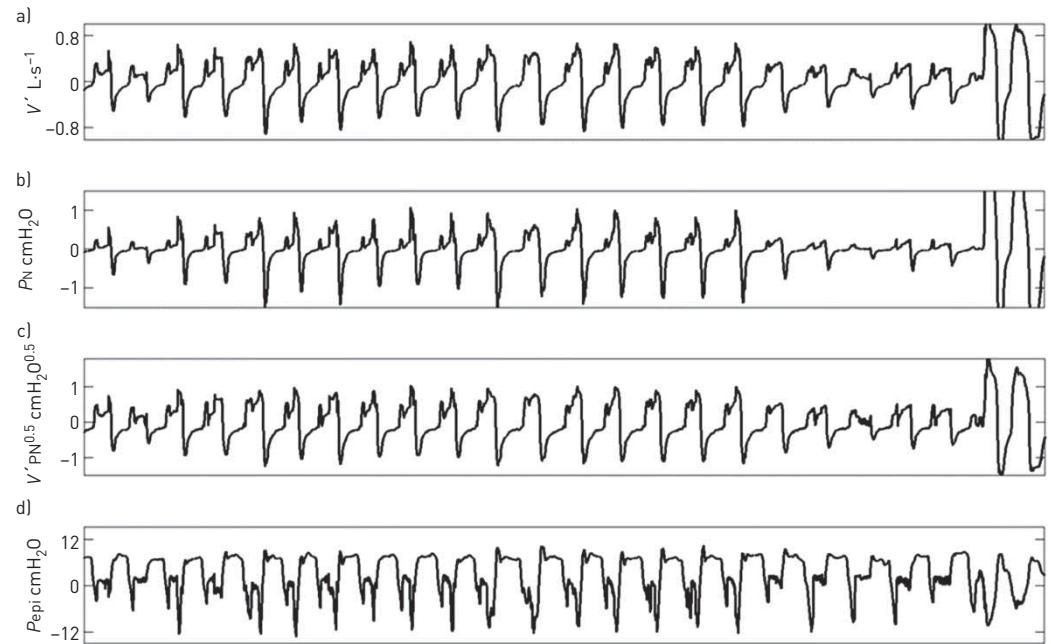


FIGURE 5 The discontinuity and jaggedness features associated with epiglottic collapse were reliably captured using a nasal cannula. These features were preserved in these example breaths that were simultaneously collected using a) a pneumotachograph (V') and b) a nasal cannula (P_N); c) to estimate the pneumotach flow, the nasal pressure signal was passed through a square root transformation ($V' P_N^{0.5}$); d) the pressure above the epiglottis (P_{epi}), indicating epiglottic collapse.

patients. However, they did not try to correlate these shapes with anatomical structures within the airway. The results of the present study show that epiglottic collapse is associated with distinct flow shapes that can be quantified objectively. As described in our recent study, a cardinal feature of epiglottic collapse is the fact that it is intermittent [17]. In addition to its intermittency, this study shows that the most important feature distinguishing epiglottic collapse from other types of airway collapse is the presence of discontinuities in the flow (quantified by the discontinuity and jaggedness indices). Both of these features quantify the rapid decrease/increase in the airflow. Indeed, in the breaths examined in this study, the collapse of the epiglottis was observed to be severe and abrupt. In particular, anteroposterior movement of the epiglottis tended to be fast and unpredictable (online supplementary video), occurring intermittently for unknown reasons. These characteristic movements produced sharp and severe reductions in airflow (figure 2) that were captured by the discontinuity index proposed in this study. In addition, the epiglottis was observed to be an unstable structure that would sometimes reopen/close repeatedly during inspiration, causing a jagged flow (figure 2 and online supplementary video). These “unstable” movements were captured by both the discontinuity and jaggedness indices.

In addition to producing unique flow features, epiglottic collapse may generate characteristic sounds that may be different than the nonepiglottic snoring sounds. Previous studies have reported a low prevalence of epiglottis-related snoring among OSA patients [29, 30]. This, at least in our study, may be due to the fact that when the epiglottis collapses, particularly in the anteroposterior direction, the collapse is abrupt and thus the “classical” snoring sound may not be generated.

Discontinuity

This feature measures the slope of the steepest line fitted to the middle portion of the inspiratory airflow (after excluding trivial fast increases/decreases in flow at the start and end of inspiration). Figure 2 demonstrates a library of breaths with epiglottic collapse in which discontinuity (or very steep increases/decreases in flow) stands out as a signature of epiglottic collapse. The discontinuity index ($D1$), described in this study, reliably quantifies these fast flow variations. Additionally, detecting changepoints before measuring the slopes adds to the reliability of this measure by making it less sensitive to fast (low amplitude) fluctuations that are present when there is fluttering (figure 3 and online supplementary figure S1).

Jaggedness

The second important characteristic that is associated with epiglottic collapse is the presence of jaggedness in both inspiration and expiration. The jaggedness indices described in this study quantify the deviation of

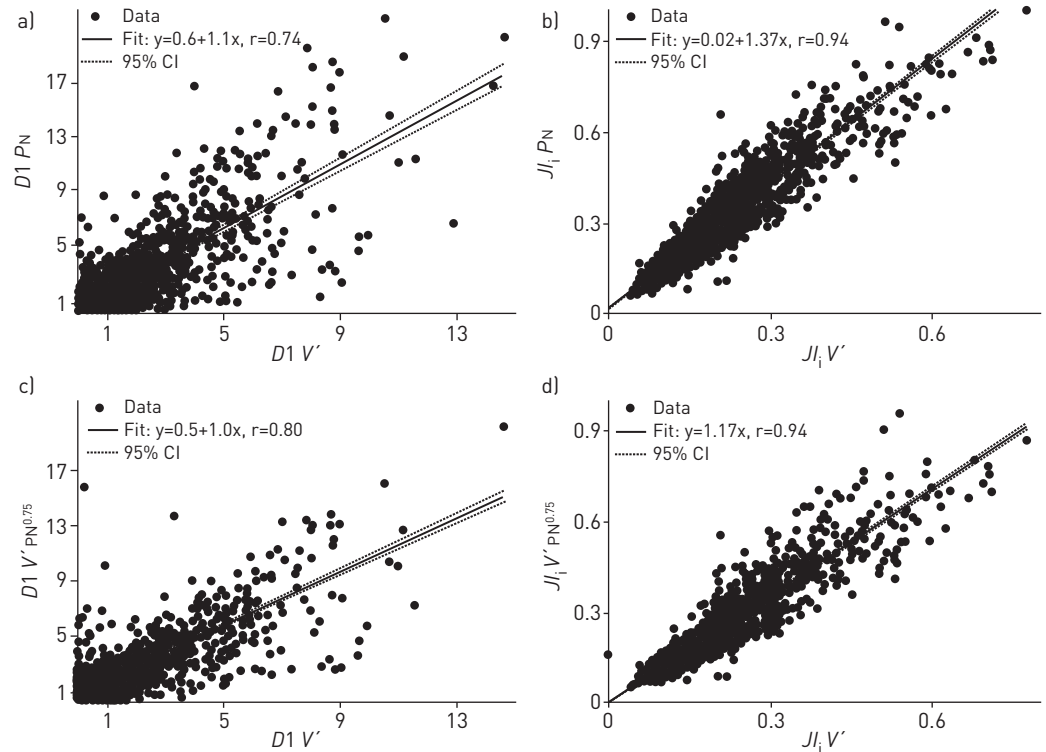


FIGURE 6 The a, c) discontinuity and b, d) jaggedness features obtained from pneumotachograph measured flow [V'] were strongly correlated with their corresponding values obtained from nasal pressure [PN]. A stronger correlation was obtained when nasal pressure was c) transformed [$V'PN^{0.75}$], compared with a) untransformed nasal pressure [PN].

the airflow (inspiratory or expiratory) from a flat reference (mean airflow), as a result, the more variable the airflow around the mean, the higher the jaggedness index (figure 4). This feature has been used by TESCHLER *et al.* [31] for automated CPAP-titration studies. In this study, we modified this feature by normalising it to the inspiratory time to take into account the subject-specific differences in inspiratory time.

Reduced tidal volume

Selected features, including inspiratory fluttering index (FP_i/V_T^2), V'_{mean}/V_T and V'_{maxE}/V_T were normalised by tidal volume and therefore are both a measure of the numerator and the tidal volume. A Wilcoxon signed rank test revealed that breaths associated with epiglottic collapse had lower tidal volume than nonepiglottic breaths (0.26 ± 0.15 L versus 0.31 ± 0.15 L; $p < 0.0001$). In addition to quantifying the tidal volume, these features measure relative mean inspiratory flow, fluttering power (between 5 Hz and 125 Hz) and peak expiratory flow, which resulted in an increase of 8% in cross-validated accuracy.

Validation against nasal pressure-measured flow

We used pneumotachograph-measured flow to develop the algorithm. However, since we hope this methodology will be adopted as a clinical tool, we validated it against high-fidelity nasal pressure signals (unfiltered, DC-coupled amplification) which can feasibly be assessed clinically. The utility of nasal pressure airflow can be witnessed by the observed identity relationships (slope of linear fit ≈ 1) and strong correlations between pneumotachograph-measured flow features and nasal pressure features (figure 6). Of note, we used flow features that do not depend on absolute (calibrated) values of pneumotachograph-measured flow to facilitate implementation with uncalibrated flow signals.

Remaining challenges for clinical use

The algorithm developed in this study automatically scores each breath as being associated with epiglottic or nonepiglottic collapse, yet ultimately these results require translation from “breath level” to a “patient level” for clinical decision making. Summarising breath-level data for an individual patient may be achieved by reporting the proportion of breaths with epiglottic collapse observed during sleep (per state or

per position), or the proportion of scored obstructive respiratory events (hypopnoeas) with epiglottic collapse. The optimal approach will be the one that best predicts responses to therapies.

Indeed, available evidence indicates that identifying the epiglottic collapse has important implications for OSA management [9, 32]. The method developed in this study can be used to test whether epiglottic collapse, assessed using this approach, predicts responses to therapy, including failure of oral appliances [9], surgery [33], increased occurrence of collapse on CPAP [10, 11, 32] and effectiveness of positional therapy [17, 32]. In addition, its utility as a screening tool for epiglottis-related surgery can be tested.

Limitations

This study has several limitations. First, due to the invasiveness of the study and the inherent challenges in performing endoscopy during natural sleep in OSA patients, our sample size was relatively modest (n=23). Nevertheless, the number of breaths (n=1232) examined was large enough that different flow patterns were equally well represented. Importantly, in the cross-validation framework, the number of features (n=7) was far less than the number of observations (n=123 in each fold), which made the training procedure more robust. Furthermore, 10-fold cross-validation was also used to prevent overfitting, which occurs when the sample size is small. Second, the number of breaths analysed was different between subjects, which could potentially bias the algorithm towards patients with more breaths. However, this was dealt with in two ways. First, the 10-fold cross-validation framework allows for the “rare cases” to be left out of the analysis and be tested with the model built with the majority cases. If the model was biased towards the majority cases, it would result in lower overall accuracy. In this study, a 3% difference was observed between classification accuracy (when the model was built and tested using the whole dataset) and cross-validation accuracy (when the model was built using 90% of the data and was tested on the remaining 10%), which suggests that if the algorithm were to be tested on a new dataset, the potential loss of accuracy would be ~3%. Second, linear mixed effect models for selected features show that three out of seven selected features are significantly different between the two groups.

A third limitation relates to the storage of large video files during endoscopy. For every minute of recording, the system produced ~1.1 GB of data, which limited our ability to store the video files continuously throughout the night. Nevertheless, we recorded an average of 148±49 min of endoscopic images per subject from the first and second halves of the night to have a well-represented library of different sites of collapse/flow patterns. In addition, the video files were stored in small files every 5–10 min to prevent missing frames and desynchronisation between the signals and videos. The final limitation is that the presence of inspiratory flow is required for the algorithm to function properly. Therefore, the method presented here would not identify epiglottic collapse in a patient whose respiratory events were mostly apnoeas.

Conclusions

In this study, an automated algorithm was developed to objectively identify breaths with epiglottic collapse as distinct from other sites of collapse. We demonstrate that an epiglottic contribution to OSA is characterised by the presence of discontinuity and jaggedness. Since the presence of epiglottic collapse seen using endoscopy has implications for success *versus* failure of OSA therapies [9–11, 32, 33], we envisage that our algorithm will enable rapid, noninvasive identification of epiglottic involvement without requiring invasive endoscopy.

References

- 1 Young T, Peppard PE, Gottlieb DJ. Epidemiology of obstructive sleep apnea: a population health perspective. *Am J Respir Crit Care Med* 2002; 165: 1217–1239.
- 2 Colt HG, Hass H, Rich GB. Hypoxemia *vs* sleep fragmentation as cause of excessive daytime sleepiness in obstructive sleep apnea. *Chest* 1991; 100: 1542–1548.
- 3 Davies CW, Crosby JH, Mullins RL, *et al.* Case-control study of 24 hour ambulatory blood pressure in patients with obstructive sleep apnoea and normal matched control subjects. *Thorax* 2000; 55: 736–740.
- 4 Kezirian EJ, Hohenhorst W, de Vries N. Drug-induced sleep endoscopy: the VOTE classification. *Eur Arch Otorhinolaryngol* 2011; 268: 1233–1236.
- 5 Vroegop AV, Vanderveken OM, Boudewyns AN, *et al.* Drug-induced sleep endoscopy in sleep-disordered breathing: report on 1,249 cases. *Laryngoscope* 2014; 124: 797–802.
- 6 Ravesloot MJ, de Vries N. One hundred consecutive patients undergoing drug-induced sleep endoscopy: results and evaluation. *Laryngoscope* 2011; 121: 2710–2716.
- 7 Lan MC, Liu SY, Lan MY, *et al.* Lateral pharyngeal wall collapse associated with hypoxemia in obstructive sleep apnea. *Laryngoscope* 2015; 125: 2408–2412.
- 8 Cavaliere M, Russo F, Iemma M. Awake *versus* drug-induced sleep endoscopy: evaluation of airway obstruction in obstructive sleep apnea/hypopnoea syndrome. *Laryngoscope* 2013; 123: 2315–2318.
- 9 Kent DT, Rogers R, Soose RJ. Drug-induced sedation endoscopy in the evaluation of osa patients with incomplete oral appliance therapy response. *Otolaryngol Head Neck Surg* 2015; 153: 302–307.

- 10 Verse T, Pirsig W. Age-related changes in the epiglottis causing failure of nasal continuous positive airway pressure therapy. *J Laryngol Otol* 1999; 113: 1022–1025.
- 11 Shimohata T, Shinoda H, Nakayama H, *et al.* Daytime hypoxemia, sleep-disordered breathing, and laryngopharyngeal findings in multiple system atrophy. *Arch Neurol* 2007; 64: 856–861.
- 12 Yucel A, Unlu M, Haktanir A, *et al.* Evaluation of the upper airway cross-sectional area changes in different degrees of severity of obstructive sleep apnea syndrome: cephalometric and dynamic CT study. *AJNR Am J Neuroradiol* 2005; 26: 2624–2629.
- 13 Huon LK, Liu SY, Shih TT, *et al.* Dynamic upper airway collapse observed from sleep MRI: BMI-matched severe and mild OSA patients. *Eur Arch Otorhinolaryngol* 2016; 273: 4021–4026.
- 14 Aittokallio T, Gyllenberg M, Saaresranta T, *et al.* Prediction of inspiratory flow shapes during sleep with a mathematic model of upper airway forces. *Sleep* 2003; 26: 857–863.
- 15 Aittokallio T, Saaresranta P, Polo-Kantola O, *et al.* Analysis of inspiratory flow shapes in patients with partial upper-airway obstruction during sleep. *Chest* 2001; 119: 37–44.
- 16 Genta PR, Sands SA, Butler JP, *et al.* Airflow shape is associated with the pharyngeal structure causing OSA. *Chest* 2017. [In press <https://doi.org/10.1016/j.chest.2017.06.017>].
- 17 Marques M, Genta PR, Sands SA, *et al.* Effect of sleeping position on upper airway patency in obstructive sleep apnea is determined by the pharyngeal structure causing collapse. *Sleep* 2017; 40: zsx005.
- 18 Møller M. Supervised learning on large redundant training sets. *Int J Neural Syst* 1993; 4: 15–25.
- 19 Huang HH, Xu T, Yang J. Comparing logistic regression, support vector machines, and permanent classification methods in predicting hypertension. *BMC Proc* 2014; 8: Suppl. 1, S96.
- 20 McQuisten KA, Peek AS. Comparing artificial neural networks, general linear models and support vector machines in building predictive models for small interfering RNAs. *PLoS One* 2009; 4: e7522.
- 21 Judson R, Elloumi F, Setzer RW, *et al.* A comparison of machine learning algorithms for chemical toxicity classification using a simulated multi-scale data model. *BMC Bioinformatics* 2008; 9: 241.
- 22 Fernández-Delgado M, Cernadas E, Barro S. Do we need hundreds of classifiers to solve real world classification problems? *J Mach Learn Res* 2014; 15: 3133–3181.
- 23 Guyon I, Elisseeff A. An introduction to variable and feature selection. *J Mach Learn Res* 2003; 3: 1157–1182.
- 24 Kohavi R. A Study of Cross-Validation and Bootstrap for Accuracy Estimation and Model Selection. In: Proceedings of the 14th International Joint Conference on Artificial Intelligence. Vol. 2. Montreal, Canada, 1995; pp. 1137–1143.
- 25 Winter B. Linear Models and Linear Mixed Effects Models in R with Linguistic Applications. <http://arxiv.org/pdf/1308.5499.pdf> Date last accessed: August 4, 2017. Date last updated: August 26, 2013.
- 26 Baayen RH, Davidson DJ, Bates DM. Mixed-effects modeling with crossed random effects for subjects and items. *J Mem Lang* 2008; 59: 390–412.
- 27 da Cunha Viana A, Jr, Mendes DL, de Andrade Lemes LN, *et al.* Drug-induced sleep endoscopy in the obstructive sleep apnea: comparison between NOHL and VOTE classifications. *Eur Arch Otorhinolaryngol* 2017; 274: 627–635.
- 28 Lin HS, Rowley JA, Badr MS, *et al.* Transoral robotic surgery for treatment of obstructive sleep apnea-hypopnea syndrome. *Laryngoscope* 2013; 123: 1811–1816.
- 29 Quinn SJ, Huang L, Ellis PD, *et al.* The differentiation of snoring mechanisms using sound analysis. *Clin Otolaryngol Allied Sci* 1996; 21: 119–123.
- 30 Saunders NA, Vandeleur T, Deves J, *et al.* Uvulopalatopharyngoplasty as a treatment for snoring. *Med J Aust* 1989; 150: 177–182.
- 31 Teschler H, Berthon-Jones M, Thompson AB, *et al.* Automated continuous positive airway pressure titration for obstructive sleep apnea syndrome. *Am J Respir Crit Care Med* 1996; 154: 734–740.
- 32 Torre C, Camacho M, Liu SY, *et al.* Epiglottis collapse in adult obstructive sleep apnea: a systematic review. *Laryngoscope* 2016; 126: 515–523.
- 33 Kezirian EJ. Nonresponders to pharyngeal surgery for obstructive sleep apnea: insights from drug-induced sleep endoscopy. *Laryngoscope* 2011; 121: 1320–1326.